ACS APPLIED MATERIALS & INTERFACES

Subscriber access provided by UNIVERSITY OF PITTSBURGH

Applications of Polymer, Composite, and Coating Materials

Superhemophobic and Anti-Virofouling Coating for Mechanically Durable and Wash-Stable Medical Textiles

Anthony Galante, Sajad Haghanifar, Eric G Romanowski, Robert Shanks, and Paul W Leu

ACS Appl. Mater. Interfaces, **Just Accepted Manuscript** • DOI: 10.1021/acsami.9b23058 • Publication Date (Web): 22 Apr 2020

Downloaded from pubs.acs.org on April 27, 2020

Just Accepted

"Just Accepted" manuscripts have been peer-reviewed and accepted for publication. They are posted online prior to technical editing, formatting for publication and author proofing. The American Chemical Society provides "Just Accepted" as a service to the research community to expedite the dissemination of scientific material as soon as possible after acceptance. "Just Accepted" manuscripts appear in full in PDF format accompanied by an HTML abstract. "Just Accepted" manuscripts have been fully peer reviewed, but should not be considered the official version of record. They are citable by the Digital Object Identifier (DOI®). "Just Accepted" is an optional service offered to authors. Therefore, the "Just Accepted" Web site may not include all articles that will be published in the journal. After a manuscript is technically edited and formatted, it will be removed from the "Just Accepted" Web site and published as an ASAP article. Note that technical editing may introduce minor changes to the manuscript text and/or graphics which could affect content, and all legal disclaimers and ethical guidelines that apply to the journal pertain. ACS cannot be held responsible for errors or consequences arising from the use of information contained in these "Just Accepted" manuscripts.

is published by the American Chemical Society. 1155 Sixteenth Street N.W., Washington, DC 20036

Published by American Chemical Society. Copyright © American Chemical Society. However, no copyright claim is made to original U.S. Government works, or works produced by employees of any Commonwealth realm Crown government in the course of their duties.

Superhemophobic and Anti-Virofouling Coating for Mechanically Durable and Wash-Stable Medical Textiles

Anthony J. Galante[1], Sajad Haghanifar[1], Eric G. Romanowski[2], Robert M.Q. Shanks[2], and Paul W. Leu[1]*

[1]Department of Industrial Engineering, University of Pittsburgh, 3700 O'Hara, Benedum Hall, Pittsburgh, PA, 15261, United States

[2]Department of Ophthalmology, Charles T. Campbell Laboratory for Ophthalmic Microbiology, University of Pittsburgh School of Medicine, 203 Lothrop Street, Pittsburgh, PA 15213, United States

KEYWORDS textile, superhemophobic, blood, virus, serum

ABSTRACT: Medical textiles have a need for repellency to body fluids such as blood, urine, or sweat that may contain infectious vectors that contaminate surfaces and spread to other individuals. Similarly, viral repellency has yet to be demonstrated and long-term mechanical durability is a major challenge. In this work, we demonstrate a simple, durable and scalable coating on nonwoven polypropylene textile that is both superhemophobic and anti-virofouling. The treatment consists of polytetrafluoroethylene (PTFE) nanoparticles in a solvent thermally sintered to polypropylene (PP) microfibers which creates a robust, low surface energy, and multi-layer, multi-length scale rough surface. The treated textiles demonstrate a static contact angle of 158.3 ± 2.6° and hysteresis of 4.7 ± 1.7° for fetal bovine serum and reduce serum protein adhesion by 89.7 ± 7.3% (0.99 log reduction). The coated textiles reduce the attachment of adenovirus type 4 and 7a virions by 99.2 ± 0.2% and 97.6 ± 0.1% (2.10 and 1.62 log), respectively, compared to noncoated controls. The treated textiles provide these repellencies by maintaining a Cassie-Baxter state of wetting where the surface area in contact with liquids is reduced by an estimated 350 times (2.54 log) compared to control textiles. Moreover, the treated textiles exhibit unprecedented mechanical durability, maintaining their liquid, protein, and viral repellency after extensive and harsh abrasion and washing. The multi-layer, multi-length scale roughness provides for mechanical durability through self-similarity and the samples have high pressure stability with a breakthrough pressure of about 255 kPa. These properties highlight the potential of durable, repellent coatings for medical gowning, scrubs, or other hygiene textile applications.

1. Introduction

Textile based products used in healthcare environments range from scrubs to masks to wound sutures to implantable devices, and these products are common vessels for the spread of infectious disease.[1] Much research attention has focused on functional textile finishes for blood repellent or antimicrobial properties due to the health hazards from textiles contacting biological fluids, such as blood, urine or sweat.[1] Contact with human body fluids is a frequent hygiene issue for patients and employees in medical settings, and existing biomaterials have failed to meet clinical needs.[2,3] Increasing interest has emerged for advanced biomaterials with repellent properties that inhibit the spread of infections.[2,4] There is a need for new coatings or surfaces with a broad range of biohazard repellency that may be applied to textiles for masks, gowns, bed linens, and drapes to reduce secondary infections in healthcare settings.[5]

New strategies for creating body fluid repellent substrates consist of designing a surface with a robust Cassie-Baxter wetting state that demonstrates high contact angles and low hysteresis with blood fluid.[6,7] A robust Cassie-Baxter wetting state consists of trapping air, which is fully repellent, under the liquid creating a metastable composite liquid-air interface. This wetting state can significantly reduce the solid-liquid interfacial area and lead to superhydrophobicity, characterized by static contact angles over 150° and hysteresis less than 10° with water. Superhemophobicity, characterized by static contact angles greater than 150° and hysteresis less than 10° with blood, is more challenging to achieve since blood has ~~a~~ lower surface tension than water (about 54 mN m^{-1} as opposed to 72.1 mN m^{-1}). Blood not only transports bacteria, fungi, viruses and other pathogens that lead to healthcare associated infections, but also contains platelets and proteins dispersed in an adhesive medium which bind and chemically interact with surfaces to cause material degradation.[8,9]

A variety of strategies for promoting Cassie-Baxter wetting have been demonstrated, such as using appropriate roughening methods combined with low surface energy materials.[10–12] Superhydrophobic, nonwoven PP textiles have been created by a scalable, solvent swelling method for

repellency of blood, urine, milk, coffee and other common liquids.[13] Superhydrophobic, shrink-induced polymers and superhemophobic titanium nanotube surfaces have been shown to repel blood and specific proteins in blood, such as fibrinogen, using fluorescent labeling.[14,15]

However, repellency to virions or virus particles has yet to be demonstrated. Viruses are the most common cause of infectious diseases within indoor environments,[16] and contaminated surfaces play a key role in transmitting these diseases.[17,18] Virions are expelled into the air from breathing, coughing, or sneezing and land on surfaces, where they become active sites for spreading infections through hand or skin contamination, ingestion, or mucus membrane contact.[19–22] Personal protective equipment, such as medical masks, gloves, gowns, goggles, and face shields, are essential to guard healthcare workers, but impose a risk of virus transmission, particularly during the process of doffing.[23] Chughtai *et. al* recently showed that respiratory virus were present on the outer surface of about 1 in 10 medical masks worn by healthcare workers and may result in self-contamination.[24] Clothing has been shown to indirectly transmit virions in various environments from education[25] to healthcare.[26]

In addition, one of the major challenges for a variety of the nanostructures used to create superhydrophobic surfaces is overcoming the poor mechanical durability of these various treatments. Most superhydrophobic surfaces are easily destroyed or damaged, sometimes with just brushing with a tissue or finger touching.[27,28] Nanostructures that are used to create superhydrophobic surfaces may easily be removed by mechanical abrasion resulting in a loss of superhydrophobicity and any associated functionality.[29] Even worse, the degradation of these coatings may make them even less effective than untreated bulk materials.[30] There is a need to create surfaces that not only repel blood, serum protein, and viruses, but are mechanically durable and wash stable. Previous superhydrophobic, blood protein repellent strategies have failed to address mechanical durability challenges[8,13,15,31] or require a subsequent heat treatment to self-repair after topological damage.[32] New textile treatments should have durable performance after repeated washing cycles and mechanical abrasion from various contacts.[33]

In this work, we demonstrate a simple, scalable and mechanically durable textile treatment that endows it with blood fluid, protein and virus repellency. The coating treatment consists of low surface energy polytetrafluoroethylene (PTFE) nanoparticles in a fluorinated, low surface energy (11.9 mN m^{-1}) solvent drop cast and thermally sintered to polypropylene (PP) microfibers. We focus on a nonwoven PP textile, which is widely used in in medical and hygiene industries for products such as garments, wipes, diapers, female sanitary products, and personal protective equipment.[34] For blood fluid and protein repellency, we use fetal bovine serum (FBS), which has similar surface tension to whole blood and is a standard for representing protein content.[35,36] For virus repellency, we use non-enveloped viruses, adenovirus types 4 (HAdv4) and 7a (HAdv7a), which can represent other non-enveloped viruses such as poliovirus and rhinovirus. HAdv4 and Hadv7a are common causes of acute respiratory disease among military recruits, which can easily spread in confined areas accidentally through air and from contact with contaminated surfaces.[37,38]

The treated fabric surfaces are both superhydrophobic and superhemophobic, demonstrating a static contact angle (θ_{CA}) and contact angle hysteresis (θ_H) of 160.8 ± 2.3° and 2.8 ± 1.4° with water, and 158.3 ± 2.6° and 4.7 ± 1.7° with FBS. The superhemophobic fabrics effectively reduce attachment of FBS proteins by 89.7 ± 7.3% compared to untreated controls. In addition, the surfaces are anti-virofouling, reducing the attachment of infectious HAdv4 and Hadv7a virions by 99.2 ± 0.2% and 97.6 ± 0.1%, respectively. The attachment reduction is from a significant decrease in surface contact area with biohazardous liquids for the treated fabrics compared to untreated controls. The treated fabrics reduce contact with liquids by an estimated 350 times less surface area (2.54 log reduction) than the surface area of control fabrics.

Most importantly, the treatment demonstrates significant durability that has yet to be demonstrated in previous research on superhemophobic surfaces. The treated fabrics continue to demonstrate superhydrophobicity with water and superhemophobicity with serum after 100,000 abrasion cycles at 30 kPa pressure or 12 ultrasonic washing cycles at 32 W cm^{-2} in detergent solution. Additionally, the samples continue to reduce the attachment of FBS proteins and both types of adenovirus virions after fabrics are subject to significant abrasion or washing cycles. Here, a simple combination of low surface energy polymers and multilayer, multi-length scale roughness provides for liquid, serum protein, and virus repellency with exceptional mechanical and washing durability. The treatment method is safe, free of glues or binders and uses commercially available materials, making treated PP textiles excellent candidates for textile applications in medical, laboratory, industrial or healthcare settings to proactively reduce the surface attachment of infection biohazards.

2. Results

2.1. Surface Characterization

Figure 1 shows the simple two-step process and structure of the textile treatment method. **Figure** 1a schematically illustrates the treatment method for creating durable, protein and virus repellent textile without changing the optical appearance. The coating solution is prepared by mixing polytetrafluoroethylene (PTFE) nanoparticles in a fluorinated, low surface energy (11.9 mN m^{-1}) solvent. Lyophobic particles such as PTFE nanopowder are prone to clumping and poor uniformity during deposition treatments[39]; therefore, ultrasonication is used to disperse the colloidal solution before drop casting to improve the coverage of the coating.

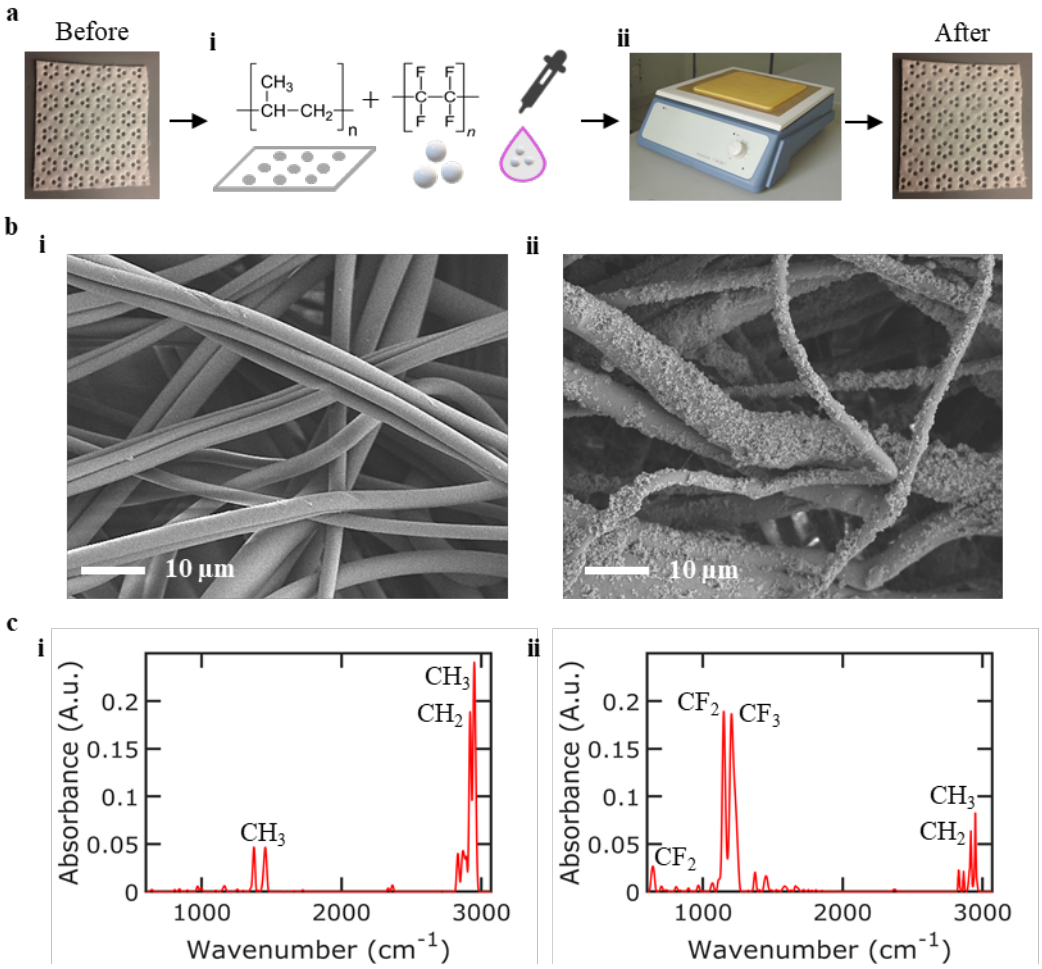

Figure 1. Process and structure of the textile treatment method using low surface energy materials. (a) Schematic illustrating the simple, two step method which does not alter the optical properties of the textile. (b) SEM images showing surface morphology of (i) untreated and (ii) treated PP textiles, respectively. (c) FTIR-ATR spectra showing chemical composition and prominent surface energy groups of (i) untreated and (ii) treated PP textiles, respectively.

Solubilizing low surface energy materials in combination with low surface tension solvents is crucial for coating repellency and durability.[40] The coating solution is drop cast onto both sides of the nonwoven textile (**Figure 1ai**), followed by a heat treatment to evaporate the solvent and thermally sinter PTFE nanoparticles to nonwoven PP microfibers (**Figure 1aii**). PTFE itself is considered inert, with low health or environmental concern;[41,42] even ingestion up to 25% of the diet is not considered a health risk.[43] The heat treatment partially softens the PP microfibers which promotes nanoparticle impregnation without causing any pyrolysis of PTFE. The solvent evaporates (boiling point of 58 °C) and eliminates any residual fluorine. After heat treatment, the textiles feel stiffer; however, cracking of the fabric coating does not occur from bending. The treatment creates robust, low surface energy, thermally bonded, multi-length scale roughened textiles.

Figure 1b compares the physical morphology of nonwoven textile before (i) and after (ii) surface treatment with images from scanning electron microscopy (SEM). Untreated samples are composed of thermally bonded PP microfibers approximately 2-8 µm in diameter (**Figure 1bi**). After treatment, exposed PP microfibers are observed to be extensively covered by

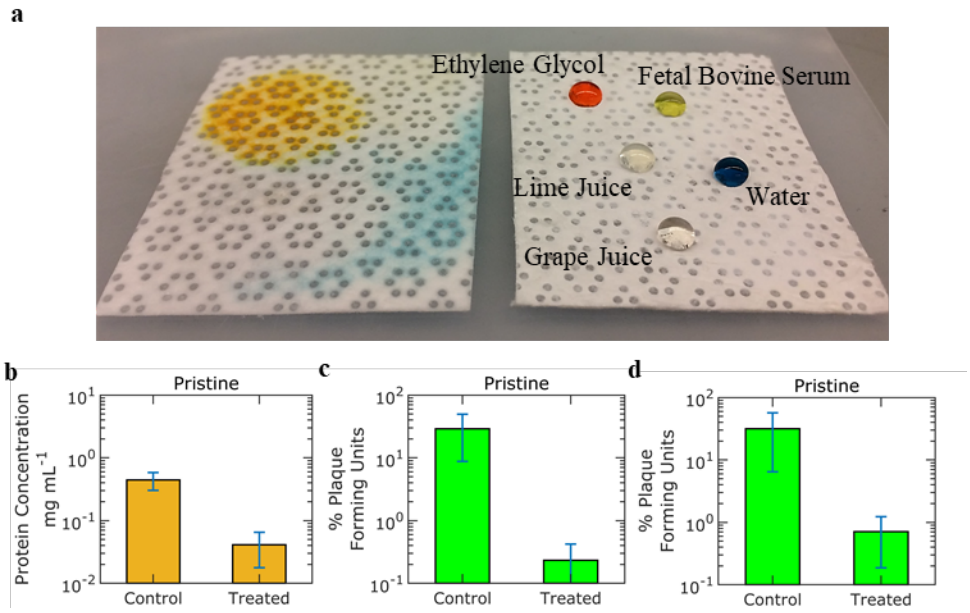

Figure 2. Liquid, protein and virus repellency results. (a) Comparison of wetting properties between control (left) and treated textile (right) with different droplets of colored test liquids. (b) Concentrations (mg mL^{-1}) of FBS protein attachment on control and treated samples after incubation. (c-d) Percent PFU of adenovirus HAdv4 (c) and Hadv7a (d) on control and treated samples after incubation.

PTFE particles approximately 250 nm in diameter (**Figure 1bii**). The coating extends onto multiple layers of the nonwoven microfiber matrix. The increased coverage of the hydrophobic PTFE nanoparticles on the hydrophobic PP microfibers creates multi-layer, multi-length scale roughness solely made of low surface energy groups important for repellency durability.

Figure 1c compares the chemical composition of textile samples before (i) and after (ii) surface treatment with Fourier transform infrared attenuated total reflectance (FTIR-ATR) spectroscopy. Untreated PP samples are dominated by peaks from CH_3 and CH_2 groups (**Figure 1ci**). After treatment, the infrared spectra of the PP textiles primarily consist of peaks from the vibrating bands of CF_3 and CF_2 groups due to the coverage of PTFE particles (**Figure 1cii**). Small peaks from CH_3 and CH_2 groups are still observed due to presence of the PP microfiber matrix. The chemical composition of low surface energy groups CF_3, CF_2, CH_3 and CH_2 potentiate the low surface energy of treated PP textiles capable for blood repelling applications.

2.2. Blood Fluid, Protein and Virus Repellency

Figure 2 highlights the repellency results of the treated textile. **Figure 2a** compares the different wetting properties between untreated and treated samples for various liquids such as water, ethylene glycol, grape juice, lime juice, and FBS. Control nonwoven textiles are fully wetting and the test liquids are absorbed into the textile. In contrast, treated textile samples are non-wetting with low hysteresis for various test liquids. Both static and dynamic contact angle measurements are performed on the treated samples to better characterize the liquid repellency of the treated surface. **Table 1** lists the static contact angle (θ_{CA}), hysteresis (θ_H), and test liquid surface tension for water and FBS from five treated textile samples reported as mean and standard deviation. The surface is both superhydrophobic with water (θ_{CA} = 160.8 ± 2.3°, θ_H = 2.8 ± 1.4°) and superhemophobic with FBS (θ_{CA} = 158.3 ± 2.6°, θ_H = 4.65 ± 1.7°). **Video S1** demonstrates the low θ_H with water and FBS by showing droplets easily rolling down the treated PP textile on a stage fixed at a 5° tilt.

Table 1. Wetting characterization of treated PP textiles with water and fetal bovine serum (FBS).

Test Liquid	Surface Tension [mN m^{-1}]	Contact Angle [°]	Hysteresis [°]
Water	72.1	160.8 ± 2.3	2.8 ± 1.4
FBS	55.7	158.3 ± 2.6	4.65 ± 1.7

FBS protein concentration (mg mL^{-1}) is characterized by UV absorbance at 280 nm for phenylalanine and tryptophan amino acids to quantify the overall content of albumin, globulin and regulatory proteins. These proteins range in size from < 1 to 10 nanometers. **Figure 2b** shows the results of the FBS protein adhesion tests on the samples after incubation. The treated surface demonstrates an 89.7 ± 7.3% decrease (0.99 ± 0.03 log reduction) of FBS protein adhesion.

The amount of virions that cause respiratory infection is quantitated in percent of plaque forming units (PFU) from adenovirus titers (PFU mL^{-1}), using standard plaque assays with human lung carcinoma cells prepared in tissue culture plates.[44,45] These virions range from 70 to 100 nm in size.[46] **Figure 2c** and **2d** show the adenovirus adhesion results for HAdv4 and Hadv7a, respectively. The treated samples demonstrate a decrease of 99.2 ± 0.2% and 97.6 ± 0.1% (2.10 and 1.62 log reductions) in attached infectious HAdv4 and Hadv7a virions versus untreated samples.

Young is credited for describing the wetting contact angle related to the interfacial energies involved in the three phase system of a perfectly smooth surface in contact with

a liquid as $cos\theta_Y = \frac{\gamma_{SV}-\gamma_{SL}}{\gamma_{LV}}$, where θ_Y is the equilibrium contact angle of a flat surface and $\gamma_{SV}, \gamma_{SL}, \gamma_{LV}$ are the corresponding surface tensions of the surface-air, solid-liquid, and liquid-air interfaces, respectively.[47] Yong further showed that at the boundary between wetting and repellent behavior, when $\theta_Y = 90°, \gamma_{SL}$ can be approximated as $\gamma_{SL} = \gamma_{SV} + \gamma_{LV} - 2\sqrt{\gamma_{SV}\gamma_{LV}}$ to obtain $\gamma_{SV} = \frac{\gamma_{LV}}{4}$.[48] Since the surface tension of natural blood is approximately $\gamma_{LV} = 52 - 56$ mN m^{-1},[5,49,50] Yong's work suggests that the free energy of a surface used for blood repellent applications should be at most $\gamma_{SV} = 13$ mN m^{-1} for creating a robust Cassie-Baxter wetting state. Using Fowkes method,[51] the surface energy of the treated textile is estimated as 12.4 mN m^{-1} (**Table S1**) due to the dominant coverage of low surface energy CF_2 and CF_3 groups.

Treated textiles reduce the attachment of blood proteins and nonenveloped virions by Cassie-Baxter wetting behavior which significantly reduces the surface area per mass in contact with liquid. The Cassie-Baxter wetting state reduces the amount of potential adhesion sites and maintains an air barrier between the substrate and potential biohazard, making adhesion more energetically difficult. Cassie-Baxter wetting is described by the equation, $cos\theta_{CA} = f_{SL}cos\theta_Y - f_{LV}$, where f_{LV} is the fractional area of

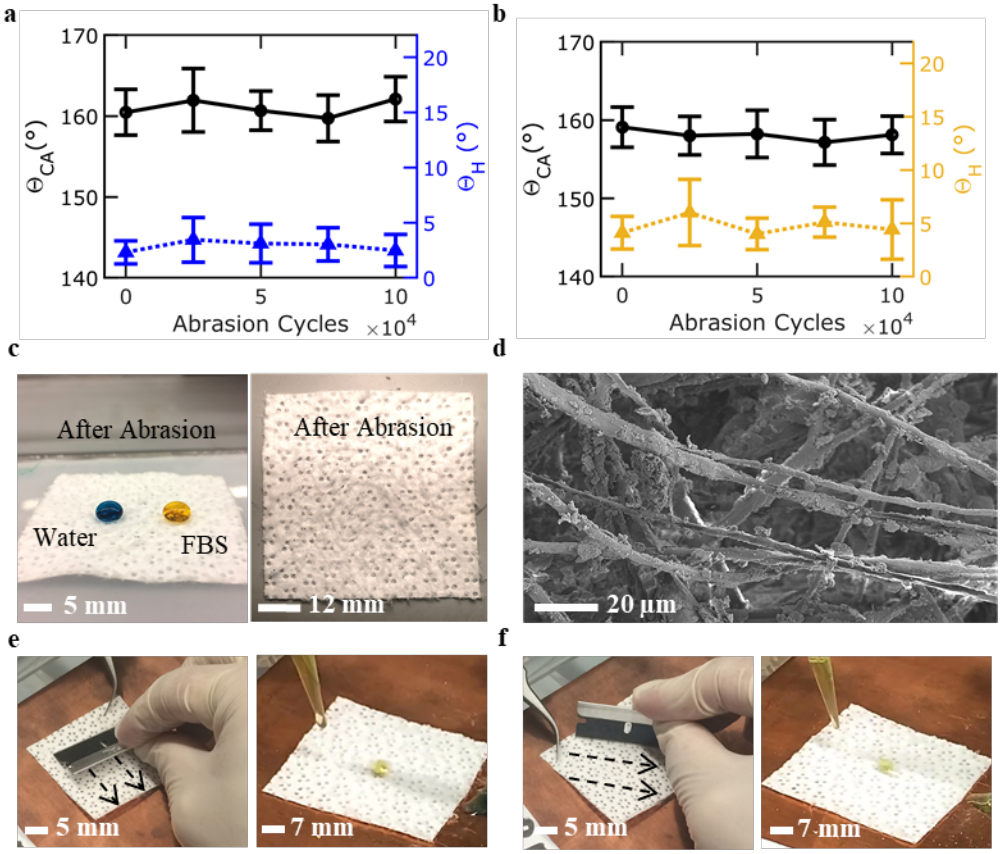

Figure 3. Mechanical abrasion durability results. (a-b) Static contact angle (left y-axes, solid black) and hysteresis (right y-axes, dotted) as a function of mechanical abrasion cycles at 30kPa pressure for (a) water (blue) and (b) FBS (orange), respectively. (c) Optical images of liquid repellency with different test liquids (right) and a representative sample (left) after 100,000 abrasion cycles. (d) SEM image of treated textiles after extensive mechanical abrasion. (e-f) Screenshots from supplemental videos showing wetting durability from razor blade abrasion and rolling FBS droplets after damage at a 5° tilt angle for (e) scraping and (f) slicing abrasion, respectively.

the liquid-vapor interface, θ_{CA} is the apparent contact angle and θ_Y is the equilibrium contact angle. The fractional area of the solid-liquid interface and the liquid-vapor interface add up to 1, $f_{SL} + f_{LV} = 1$. The fractional area of the solid-liquid interface f_{SL} is estimated by measuring the apparent and equilibrium contact angles of 4 different liquids with known surface tensions γ_{LV}: water (72.1 mN m^{-1}), FBS (55.7 mN m^{-1}), ethylene glycol (47.3 mN m^{-1}) and hexadecane (27.3 mN m^{-1}), and using f_{SL} in the Cassie-Baxter equation as a fitting parameter (**Figure S1**). Apparent contact angles are measured on the PTFE nanoparticle treated PP textile and equilibrium contact angles are measured on a flat PTFE surface. f_{SL}= 0.14 ± 0.06 based on the curve fit, suggesting that the liquid contacts about 14% of the surface in the Cassie-Baxter state.

The available specific surface area in treated textiles for proteins or virions to attach to is estimated to be 0.2 ± 0.1 m^2 g^{-1} given that f_{SL}= 0.14 and the PP textile has a specific surface area per mass of 1.1 m^2 per gram. In contrast, the control textiles are fully wetted by liquids. The specific surface area of the control textiles is calculated by methylene blue absorption, which measures the accessible area of a surface per unit mass at the monolayer of the textile fibers.[52] The specific surface area of control textiles is estimated as

69.3 ± 16.9 m^2 g^{-1} (**Table S2**). Thus, we estimate the textile treatment reduces the surface area in contact with the liquid by about 350 times (2.54 log).

2.3. Repellency Durability

We next characterize the mechanical durability of the treated nonwoven PP textile by studying the degradation of the liquid, protein, and virus repellency reported in the previous section after mechanical abrasion and ultrasonic washing. **Figure 3** shows the liquid repellency results of the treated textile after mechanical abrasion. Superhemophobic PP textile samples are abraded by a linear abrader with a Scotch-Brite scrub attachment at an applied load pressure of 30 kPa, which is 2.5 times the pressure of typical heavy-duty upholstery tests.[39]

In **Figure 3a** and **3b**, the apparent contact angle θ_{CA} and contact angle hysteresis θ_H for water and FBS are shown for every 25,000 abrasion cycles up to 100,000, which is four times the threshold for commercial use of textiles.[53] θ_{CA} and θ_H are 162.1 ± 2.8° and 2.5 ± 1.5° for water, and 158.1 ± 2.4° and 4.4 ± 2.8° for FBS after 100,000 cycles of mechanical abrasion. For water, θ_{CA} decreases by 1.6 ± 2.7° and θ_H increases by 0.7 ± 1.0°. For serum, θ_{CA} decreases by 1.0 ± 3.4° and θ_H increases by 0.1 ± 3.1°. Small deviations in θ_{CA} and θ_H are attributed to some loss of nanoparticles after abrasion; however, repellency is maintained by a

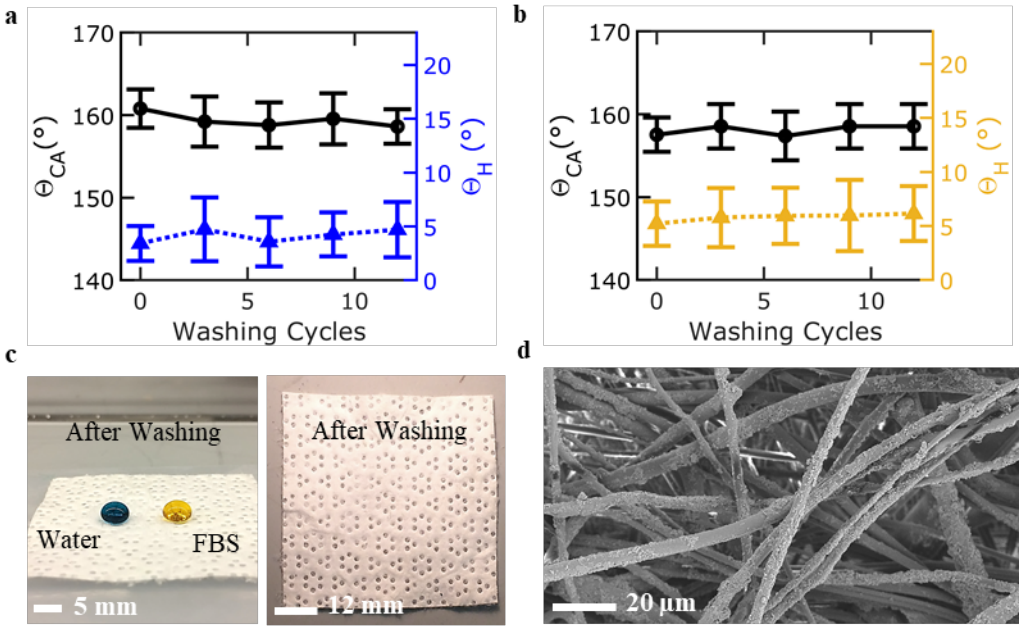

Figure 4. Ultrasonic washing durability results. (a-b) Static contact angle (left y-axis, solid black) and hysteresis (right y-axis, dotted) as a function of ultrasonic washing cycles in a detergent solution for (a) water (blue) and (b) FBS (orange). (c) Optical images of liquid repellency with different test liquids (right) and a representative sample (left) after 12 ultrasonic washing cycles. (d) SEM image of treated textiles after extensive ultrasonic washing.

roughened PP microfiber matrix. The roughening action of abrasion on low surface energy PP microfibers promotes Cassie-Baxter wetting. The hydrophobic microfiber matrix is liquid repellent when roughened, while protecting nanoparticle roughness from being abraded off. PTFE nanoparticles become mechanically trapped in the nonwoven fiber matrix. Embedded nanoparticles and roughened microfibers can be seen after extensive abrasion cycles. Representative optical and SEM images of treated textile after 100,000 abrasion cycles are shown in **Figure 3c** and **3d**.

Additionally, treated samples are durable to scratching and cross slicing abrasion with a razor blade. **Figure 3e** and **3f** show representative images of razor blade abrasion on the sample and serum droplets rolling afterwards at a 5° tilt angle. Serum and water droplets are still easily repelled at a 5° tilt angle after various razor blade scratches, crossing slices, or abrasion cycles. **Videos S2** and **S3** show droplets of both liquids rolling off treated textiles after razor blade scratching and slicing tests, respectively.

Many repellent strategies utilize fluorinated silane chemistry, such as fluorinated silica nanoparticles, which consists of fluorine chains bonded to a hydrophilic silica bulk.[53–55] However, after the fluorine molecules are rubbed off, the hydrophilic silica bulk interacting at the surface eliminates repellency.[30] In contrast, our surface treatment consists of multi-layer, multi-length scale features made solely of low surface energy groups, which maintain a robust Cassie-Baxter wetting state after mechanical abrasion for a broad range of liquids.

The mechanical robustness of the treated textile stems from its multi-layer, multi-length scale, low surface energy morphology of PTFE nanoparticles and PP microfibers. The treated substrate consists of low surface energy nanoparticles thermally bonded to low surface energy PP micron sized fibers. The nanoparticles are impregnated through multiple layers of the structure. This multi-layer nature of the surface provides for mechanical robustness as any rough abrasion to the surface, results in the exposure of a similar underlying low surface energy surface. The multi-

length scale of the surface also aids in this robustness as the PP microfibers act as protuberances that protect PTFE nanoparticle roughness from being abraded off.[56] Superhydrophobicity and superhemophobicity are thus maintained after a variety of harsh abrasion or razor blade scratching or slicing conditions. **Figure 4** shows the liquid repellency results of the treated textile after washing using an ultrasonic cleaner. Ultrasonic cleaning devices produce waves that create imploding microscopic bubbles, causing a non-abrasive scrubbing action superior to traditional cleaning methods. 0.3L of H_2O at acoustic intensity of at least 20 W cm^{-2} has been shown to have higher washing efficiency than a standard washing machine.[57] Ultrasonic washing cycles use an industrial soap detergent for heavy-duty cleaning applications to further simulate aggressive washing conditions.

Figure 4a and **4b** show the static contact angles and hysteresis for water and FBS after 12 ultrasonic washing cycles, respectively. θ_{CA} and θ_H are 158.6 ± 2.1° and 4.7 ± 2.6° for water, and 157.6 ± 2.7° and 6.1 ± 2.5° for FBS after ultrasonic washing. For water, θ_{CA} decreased by 2.2 ± 1.5° and θ_H increased by 1.3 ± 1.4°. For serum, θ_{CA} decreased by 1.0 ± 3.9° and θ_H increased by 0.9 ± 2.1°. Decreases in θ_{CA} and increases in θ_H result from a loss of nanoparticles that expose more of the microfibers, which have higher surface energy than the nanoparticles. However, nanoparticles are still observed on the microfibers after numerous washing cycles, shown by the SEM image of **Figure 4d**. **Figure 4c** shows representative optical images of treated textiles after washing. The results demonstrate that treated samples maintain a Cassie-Baxter wetting state with high static contact angle and low hysteresis with water and FBS for effective liquid repellency after washing.

In order to explain the wash stability of the Cassie-Baxter state, the breakthrough pressure, or maximum external pressure the surface can tolerate before the transition from Cassie-Baxter to Wenzel state, is measured experimentally by observing a water droplet evaporate on the surface.[7,11] The breakthrough pressure of the superhemophobic PP textile is at least 260 kPa, corresponding to a transition in wetting state when the droplet diameter is at most 560 µm (**Figure S3**). Therefore, the Cassie-Baxter state is stable up to 15 meters underwater or as long as the pressure applied by a liquid droplet is less than 260 kPa.

Figure 5 shows the biohazard repellency results after durability testing. Biohazard repellency is still observed after 100,000 abrasion cycles (abraded) and 12 ultrasonic washing cycles (washed), demonstrating a durable, protein and viral repellent textile capable of repeatable use in healthcare settings. **Figure 5a** shows FBS protein binding concentrations after incubation on abraded and washed samples. Treated textiles show 92.6 ± 1.4% and 92.7 ± 4.8% less FBS protein content than the control for abraded and washed conditions, respectively. The absolute deviations of attached protein concentration from pristine conditions are 22.8 ± 14.6 µg mL^{-1} after abrasion and 23.0 ± 15.3 µg mL^{-1} after washing. These deviations are within the range of error from background absorbance (50 µg mL^{-1}, Figure S3); therefore, we conclude the extent of protein repellency for treated textiles is the same after extensive abrasion or washing.

Figure 5b and **5c** show the percent (%) of PFU that attached to samples after incubation with adenovirus type 4 and 7a, respectively. For HAdv4, the treated textile shows 96.0 ± 4.3%, and 98.4 ± 0.9% less infectious virions than the control for abraded and washed conditions, respectively. The absolute deviation of HAdv4 virion repellency from pristine conditions is 0.2 ± 0.1% after extensive abrasion and 0.2 ± 0.1% after washing. For Hadv7a, treated textile shows 86.7 ± 11.2%, and 98.3 ± 1.6% less infectious virions than the control for abraded and washed conditions, respectively. The absolute deviation of HAdv7a virion repellency from pristine conditions is 1.1 ± 0.6% after extensive abrasion and 0.2 ± 0.1% after washing. Changes in overall percent (%) PFU are attributed to deviations in virion attachment for control samples after durability testing, not the repellency performance of the coating. We conclude the anti-virofouling performance of the treatment does not change after extensive abrasion or washing.

All in all, treated samples show durable repellency to FBS proteins and both types of adenovirus after mechanically abraded and ultrasonically washed conditions. The repellency robustness is attributed to the stability of the Cassie-Baxter state after mechanical abrasion and washing. A stable Cassie-Baxter

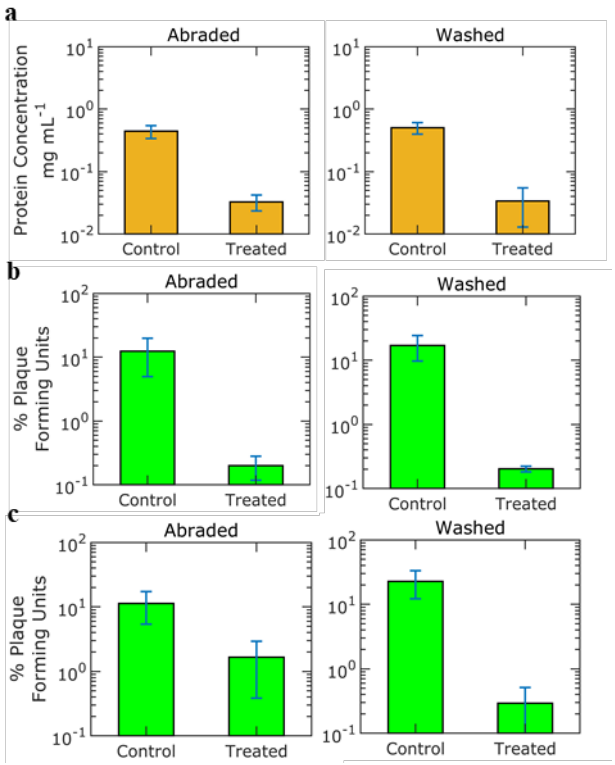

Figure 5. Protein and virus repellency durability results. (a) Concentrations (mg mL^{-1}) of FBS protein attachment on treated and control samples in mechanically abraded and washed conditions, respectively. (b) Percent PFU from adenovirus HAdv4 attached to treated and control samples in mechanically abraded and washed conditions, respectively. (c) Percent PFU from adenovirus Hadv7a attached to treated and control samples in mechanically abraded and washed conditions, respectively.

wetting state is obtained using solely low surface energy materials combined with permanent, multi-length scale

texturing for durable, blood fluid, protein and virus repellency. The extent of protein repellency is comparable to other works[15,31,32]; however, our treated textiles maintain repellency after extensive abrasion and washing. Additionally, the superhemophobic textiles are anti-virofouling, reducing the accumulation of virus particles on the surface. This work represents the first demonstration of treated textiles with reduced attachment of infectious nonenveloped virions by over 1.5 orders of magnitude, extending textile repellency for relevant biohazards that can spread disease through air and contaminated surfaces.[58]

3. Conclusion

In summary, a simple, two-step PTFE nanoparticle treatment on nonwoven microfiber PP textile can effectively repel various liquids including water and FBS. The treatment can significantly reduce the attachment of serum protein and infectious non-enveloped virions to the surface by simultaneous low surface energy and multi-length scale roughness. The repellency of test liquids, serum proteins, and adenovirus virions is maintained after significant mechanical abrasion and ultrasonic washing cycles to the fabric, which has yet to be reported. Treated fabrics may be used in healthcare, laboratory and industrial settings to proactively reduce the surface attachment of infectious biohazards. The treatment is simple, durable and uses commercially available materials, showing promise for blood-repellent and smart healthcare textile applications.

4. Experimental Section

Materials: Kimberly-Clark Professional nonwoven, thermally bonded PP textiles, acetone (99.5%), methanol (99.9%) and isopropyl alcohol (99.5%) were bought from VWR. PTFE nanopowder, tetradecafluorohexane (95%), hexadecane (98%), ethylene glycol (98%), PBS, FBS and diiodomethane (99%) were bought from Sigma-Aldrich. Extran MN 01 powdered detergent was purchased from MilliporeSigma. Deionized water was used from a Millipore Academic A10 system with total organic carbon below 40 ppb. Adenovirus type 4 and adenovirus type 7a were obtained from the American Type Culture Collection (ATCC), Manassas, VA. Adenovirus stocks in PBS were prepared with A549 human lung carcinoma cells and were cesium chloride centrifugation purified to remove any cellular and FBS proteins. The virus stocks were diluted in sterile PBS to the experimental titers used.

Sample Preparation: 0.5 in. by 0.5 in. square samples were cut from Kimtech PP textiles. All samples were rinsed with acetone, methanol and isopropyl alcohol and dried with nitrogen to eliminate possible contaminants. Coating solution was obtained by mixing PTFE nanoparticles (10 mg mL^{-1}) in tetradecafluorohexane solvent and sonicating for 30 minutes to form a stable, homogeneous dispersion prior to coating. Treated samples were heated and soaked in ethanol prior to drop casting to improve nanoparticle dispersion and deposition. Then, the nanoparticle solution was added dropwise onto both sides of the wetted substrate to fully cover the textile, followed by a thermal casting treatment on both sides at 130°C for 30 minutes on a hot plate. Lastly, unadhered PTFE particles were washed off with ethanol and the samples were dried with nitrogen.

Sample Characterization: The physical morphologies of PP surfaces were characterized by scanning electron microscopy (SEM, Zeiss Sigma 500 VP) at 5kV. For SEM imaging, all samples were sputter coated with 10 nm gold/palladium (80:20) using a sputter coater (Denton). The chemical compositions of PP samples were characterized by Fourier transform infrared spectroscopy (FTIR, Bruker Vertex-70LS) between 600 and 3200 cm^{-1} wavelengths. Untreated PP samples had peaks at 2955 cm^{-1} and 2873 cm^{-1} to attribute to asymmetric and symmetric CH_3 groups, 2922 cm^{-1} and 2843 cm^{-1} due to asymmetric and symmetric CH_2 groups, 1460 cm^{-1} and 1378 cm^{-1} from scissor or deformation CH_3 vibrating bands, and multiple peaks between 1200-750 cm^{-1} from C-H wagging, C-C asymmetric and symmetric groups and CH_3 asymmetric rocking. The infrared spectra of treated PP textile was dominated by vibrating bands CF_3 at 1213 cm^{-1}, CF_2 at 1155 cm^{-1} and 639 cm^{-1} from the coverage of PTFE particles.

Static, advancing and receding contact angle measurements were taken in ambient air at 22–25°C and 20–30% relative humidity using an optical tensiometer (Attension, 811 Theta). 5 µL droplets at 25°C for all test liquids were used for all wetting measurements. The hysteresis was tabulated for each treatment after measuring the advancing and receding contact angles during syringe-controlled water dispersion and withdrawal, respectively.

For treated textiles, the fractional surface area, f_{SL} , was estimated by measuring static contact angles of 4 different liquids with different surface tensions: water (72.1 mN m^{-1}), FBS (55.6 mN m^{-1}), ethylene glycol (47.1 mN m^{-1}) and hexadecane (27.3 mN m^{-1}). Apparent contact angles were measured on the PTFE nanoparticle treated PP textile. Equilibrium contact angles were measured on a flat PTFE surface, assuming the PP microfibers are fully covered by PTFE nanoparticles. The apparent contact angle and equilibrium contact angles were plotted and compared to a Cassie-Baxter model. f_{SL} is used as a fitting parameter, and the curve fit is shown for f_{SL} = 0.14 ± 0.06 in **Figure S1**.

Fowkes method was used to estimate the total surface free energy of the treated PP textile with water and a purely dispersive liquid, diiodomethane. The independent dispersion and polar surface energy components for each sample group were calculated using Young's and Dupre's definition of adhesion equations.[59] The apparent contact angles of the two test liquids were used to quantify the Young's contact angles using the fitted f_{SL} and roughness parameter of 2.0 from ImageJ analysis. Then, the Young's angles were used to calculate the polar and dispersive surface energy components. These quantities were summed for the overall surface free energy. Important values from these calculations are shown in **Table S1**.

Breakthrough pressure was measured by observing the contact angle and volume while a water droplet evaporates, as shown in **Figure S2**.[60] When the droplet transitioned from Cassie-Baxter to Wenzel state the diameter of the droplet was tabulated to calculate the breakthrough pressure.

For control textiles, specific surface area was measured using methylene blue absorption.[52] 6 samples of 2 g PP textiles were cut, cleaned with organic alcohol and immersed in 0.0002 mol L^{-1} methylene blue/deionized water for 24

hours. Methylene blue absorption was measured at 660 nm using a spectrophotometer (PerkinElmer, Lambda 750) to observe an absorption isotherm. The specific surface area is calculated once a monolayer is absorbed on the fibers. Measurements from the specific surface area calculations are shown in **Table S2**.

Serum Protein and Adenovirus Assay: Textile samples were completely submerged in 0.4 mL of FBS or adenovirus/PBS in Eppendorf tubes with moderate shaking for 30 minutes (Stoval Belly Dancer, level 5) at room temperature. Adenovirus/PBS inoculum titers were averaged as $1.6x10^5$ and $1.4x10^4$ PFU mL^{-1} for types 4 and 7a viruses, respectively. After shaking, samples were gingerly rinsed twice in sterile PBS and submerged in Eppendorf tubes with 0.3 mL of PBS. Then, serum proteins or virions attached on the surface were removed from the samples into PBS by sonication at power 8 for 10 seconds (Qsonica, Model Q55) within the tubes. Then, protein concentrations (mg mL^{-1}) were measured by UV absorbance at 280 nm wavelengths with a spectrophotometer (Nanodrop, model 2000) from 2 μL droplets of the PBS following sonication. Samples submerged in PBS only were used to identify potential UV absorbance interference or background, as shown in **Figure S3**.

Adenovirus titers (PFU mL^{-1}) were determined using standard plaque assay with A549 human lung carcinoma cells prepared in 24-well tissue culture plates.[44,45] After 6-7 days incubation at 37°C in 5% CO_2, the cells were fixed and stained with gentian violet prepared in formalin, the number of plaques per well were counted under a dissecting microscope, and viral plaque forming unit titers were calculated.[44,45] Percent (%) PFU was calculated using averaged adenovirus titers (PFU mL^{-1}). Finally, right-tailed Mann-Whitney U-tests rejected the null hypothesis at p values < 0.05 for all comparisons between control and treated samples.

Durability Testing: Mechanical abrasion tests were performed using Taber Linear Abrader (Model 5750) under Ford Laboratory Test Method standards for resistance to abrasion of textile treatments (BN 108-02). A Scotch-Brite scrub attachment was applied under 30kPa of pressure at a constant speed of 60 cycles per minute. Samples were fixed on a stage and subject to abrasion cycles. Additional representative SEM images of samples after abrasion are shown in **Figure S4**.

Washing cycles were performed using a Powersonic P230 Ultrasonic Cleaner (Crest) under ASTM G131-96 standards for washing materials by ultrasonic techniques. 200 mL of H_20 and 0.5 g of Extran MN 01 powdered detergent were mixed in a 500 mL beaker to create a highly efficient washing solution. Samples were submerged by 2 mL of solution in Eppendorf tubes and ultrasonicated for 40 minutes at 80 W and 49°C to complete one wash cycle. Afterwards, samples were dried in ambient temperature before testing.

Supplementary Videos: All videos were carried out on a stage fixed at a 5° tilt angle. Hysteresis of water and FBS from 0.5 mL droplets on pristine treated textiles was demonstrated in **Video S1**. **Video S2** showed the durability of test liquid hysteresis after aggressive scratching with a razor blade across the surface. **Video S3** showed the durability of test liquid hysteresis after diagonal razor blade cross slicing along the surface.

ASSOCIATED CONTENT

Supporting Information. Fractional surface area model fitting, surface energy calculations, images of breakthrough pressure experiment, representative SEM images after abrasion, and all supplementary videos. This material is available free of charge via the Internet at http://pubs.acs.org.

AUTHOR INFORMATION

Corresponding Author

* E-mail: pleu@pitt.edu

Author Contributions

The manuscript was written through contributions of all authors. All photos/graphics were taken/created by the first author.

ACKNOWLEDGMENT

This work was supported by the University of Pittsburgh. The authors would also like to acknowledge Nicholas A. Stella for his helpful discussion in the protein and viral repellency testing.

REFERENCES

(1) Gokarneshan, N. A Review of Some Recent Breakthroughs in Medical Textiles Research. *Curr. Trends Fash. Technol. Text. Eng.* **2018**, *2*. https://doi.org/10.19080/CTFTTE.2018.02.555588.

(2) Sotiri, I.; Robichaud, M.; Lee, D.; Braune, S.; Gorbet, M.; Ratner, B. D.; Brash, J. L.; Latour, R. A.; Reviakine, I. BloodSurf 2017: News from the Blood-Biomaterial Frontier. *Acta Biomater.* **2019**, *87*, 55–60. https://doi.org/10.1016/j.actbio.2019.01.032.

(3) Hedayati, M.; Neufeld, M. J.; Reynolds, M. M.; Kipper, M. J. The Quest for Blood-Compatible Materials: Recent Advances and Future Technologies. *Mater. Sci. Eng. R Rep.* **2019**, *138*, 118–152. https://doi.org/10.1016/j.mser.2019.06.002.

(4) Black, S. Trends in Smart Medical Textiles. In *Smart Textiles for Medicine and Healthcare - Materials, systems and applications*; Van Langenhove, L., Ed.; Woodhead Publishing Ltd.: Cambridge, 2007; pp 3–26.

(5) Lee, S.; Cho, J.-S.; Cho, G. Antimicrobial and Blood Repellent Finishes for Cotton and Nonwoven Fabrics Based on Chitosan and Fluoropolymers: *Text. Res. J.* **2016**. https://doi.org/10.1177/004051759906900205.

(6) Jokinen, V.; Kankuri, E.; Hoshian, S.; Franssila, S.; Ras, R. H. A. Superhydrophobic Blood-Repellent Surfaces. *Adv. Mater.* **2018**, *30* (24), 1705104. https://doi.org/10.1002/adma.201705104.

(7) Haghanifar, S.; Tomasovic, L. M.; Galante, A. J.; Pekker, D.; Leu, P. W. Stain-Resistant, Superomniphobic Flexible Optical Plastics Based on Nano-Enoki Mushroom-like Structures. *J. Mater. Chem. A* **2019**, *7* (26), 15698–15706. https://doi.org/10.1039/C9TA01753D.

(8) Leszczak, V.; Smith, B. S.; Popat, K. C. Hemocompatibility of Polymeric Nanostructured Surfaces. *J. Biomater. Sci. Polym. Ed.* **2013**, *24* (13), 1529–1548. https://doi.org/10.1080/09205063.2013.777228.

(9) Tang, L.; Hu, W. Molecular Determinants of Biocompatibility. *Expert Rev. Med. Devices* **2005**, *2* (4), 493–500. https://doi.org/10.1586/17434440.2.4.493.

(10) Kota, A. K.; Mabry, J. M.; Tuteja, A. Superoleophobic Surfaces: Design Criteria and Recent Studies. *Surf. Innov.*

2013, *1* (2), 71–83. https://doi.org/10.1680/si.12.00017.

(11) Haghanifar, S.; McCourt, M.; Cheng, B.; Wuenschell, J.; Ohodnicki, P.; Leu, P. W. Creating Glasswing Butterfly-Inspired Durable Antifogging Superomniphobic Supertransmissive, Superclear Nanostructured Glass through Bayesian Learning and Optimization. *Mater. Horiz.* **2019**. https://doi.org/10.1039/C9MH00589G.

(12) Kayes, M. I.; Galante, A. J.; Stella, N. A.; Haghanifar, S.; Shanks, R. M. Q.; Leu, P. W. Stable Lotus Leaf-Inspired Hierarchical, Fluorinated Polypropylene Surfaces for Reduced Bacterial Adhesion. *React. Funct. Polym.* **2018**, *128*, 40–46. https://doi.org/10.1016/j.reactfunctpolym.2018.04.013.

(13) Zhu, T.; Cai, C.; Duan, C.; Zhai, S.; Liang, S.; Jin, Y.; Zhao, N.; Xu, J. Robust Polypropylene Fabrics Super-Repelling Various Liquids: A Simple, Rapid and Scalable Fabrication Method by Solvent Swelling. *ACS Appl. Mater. Interfaces* **2015**, *7* (25), 13996–14003. https://doi.org/10.1021/acsami.5b03056.

(14) Movafaghi, S.; Leszczak, V.; Wang, W.; Sorkin, J. A.; Dasi, L. P.; Popat, K. C.; Kota, A. K. Hemocompatibility of Superhemophobic Titania Surfaces. *Adv. Healthc. Mater.* **2017**, *6* (4), 1600717. https://doi.org/10.1002/adhm.201600717.

(15) Nokes, J. M.; Liedert, R.; Kim, M. Y.; Siddiqui, A.; Chu, M.; Lee, E. K.; Khine, M. Reduced Blood Coagulation on Roll-to-Roll, Shrink-Induced Superhydrophobic Plastics. *Adv. Healthc. Mater.* **2016**, *5* (5), 593–601. https://doi.org/10.1002/adhm.201500697.

(16) Barker, J.; Stevens, D.; Bloomfield, S. F. Spread and Prevention of Some Common Viral Infections in Community Facilities and Domestic Homes. *J. Appl. Microbiol.* **2001**, *91* (1), 7–21. https://doi.org/10.1046/j.1365-2672.2001.01364.x.

(17) Boone, S. A.; Gerba, C. P. Significance of Fomites in the Spread of Respiratory and Enteric Viral Disease. *Appl. Environ. Microbiol.* **2007**, *73* (6), 1687–1696. https://doi.org/10.1128/AEM.02051-06.

(18) Lei, H.; Li, Y.; Xiao, S.; Yang, X.; Lin, C.; Norris, S. L.; Wei, D.; Hu, Z.; Ji, S. Logistic Growth of a Surface Contamination Network and Its Role in Disease Spread. *Sci. Rep.* **2017**, *7* (1), 1–10. https://doi.org/10.1038/s41598-017-13840-z.

(19) Abad, F. X.; Pintó, R. M.; Bosch, A. Survival of Enteric Viruses on Environmental Fomites. *Appl. Environ. Microbiol.* **1994**, *60* (10), 3704–3710.

(20) Bellamy, K.; Laban, K. L.; Barrett, K. E.; Talbot, D. C. S. Detection of viruses and body fluids which may contain viruses in the domestic environment /core/journals/epidemiology-and-infection/article/detection-of-viruses-and-body-fluids-which-may-contain-viruses-in-the-domestic-environment/56CCDAD479AFD0D35830772853F33ADD (accessed Oct 28, 2019). https://doi.org/10.1017/S0950268898001678.

(21) Tuladhar, E.; Hazeleger, W. C.; Koopmans, M.; Zwietering, M. H.; Beumer, R. R.; Duizer, E. Residual Viral and Bacterial Contamination of Surfaces after Cleaning and Disinfection. *Appl. Environ. Microbiol.* **2012**, *78* (21), 7769–7775. https://doi.org/10.1128/AEM.02144-12.

(22) Otter, J. A.; Yezli, S.; French, G. L. The Role of Contaminated Surfaces in the Transmission of Nosocomial Pathogens. *Use Biocidal Surf. Reduct. Healthc. Acquir. Infect.* **2014**, 27–58. https://doi.org/10.1007/978-3-319-08057-4_3.

(23) Katoh, I.; Tanabe, F.; Kasai, H.; Moriishi, K.; Shimasaki, N.; Shinohara, K.; Uchida, Y.; Koshiba, T.; Arakawa, S.; Morimoto, M. Potential Risk of Virus Carryover by Fabrics of Personal Protective Gowns. *Front. Public Health* **2019**, *7*. https://doi.org/10.3389/fpubh.2019.00121.

(24) Chughtai, A. A.; Stelzer-Braid, S.; Rawlinson, W.; Pontivivo, G.; Wang, Q.; Pan, Y.; Zhang, D.; Zhang, Y.; Li, L.; MacIntyre, C. R. Contamination by Respiratory Viruses on Outer Surface of Medical Masks Used by Hospital Healthcare Workers. *BMC Infect. Dis.* **2019**, *19* (1), 491. https://doi.org/10.1186/s12879-019-4109-x.

(25) IKEDA, K.; TSUJIMOTO, K.; SUZUKI, Y.; KOYAMA, A. H. Survival of Influenza A Virus on Contaminated Student Clothing. *Exp. Ther. Med.* **2015**, *9* (4), 1205–1208. https://doi.org/10.3892/etm.2015.2278.

(26) Sakaguchi, H.; Wada, K.; Kajioka, J.; Watanabe, M.; Nakano, R.; Hirose, T.; Ohta, H.; Aizawa, Y. Maintenance of Influenza Virus Infectivity on the Surfaces of Personal Protective Equipment and Clothing Used in Healthcare Settings. *Environ. Health Prev. Med.* **2010**, *15* (6), 344–349. https://doi.org/10.1007/s12199-010-0149-y.

(27) Groten, J.; Rühe, J. Surfaces with Combined Microscale and Nanoscale Structures: A Route to Mechanically Stable Superhydrophobic Surfaces? *Langmuir* **2013**, *29* (11), 3765–3772. https://doi.org/10.1021/la304641q.

(28) Milionis, A.; Loth, E.; Bayer, I. S. Recent Advances in the Mechanical Durability of Superhydrophobic Materials. *Adv. Colloid Interface Sci.* **2016**, *229*, 57–79. https://doi.org/10.1016/j.cis.2015.12.007.

(29) Xue, C.-H.; Ma, J.-Z. Long-Lived Superhydrophobic Surfaces. *J. Mater. Chem. A* **2013**, *1* (13), 4146–4161. https://doi.org/10.1039/C2TA01073A.

(30) Verho, T.; Bower, C.; Andrew, P.; Franssila, S.; Ikkala, O.; Ras, R. H. A. Mechanically Durable Superhydrophobic Surfaces https://onlinelibrary.wiley.com/doi/abs/10.1002/adma.201003129 (accessed Aug 1, 2019). https://doi.org/10.1002/adma.201003129.

(31) Koc, Y.; Mello, A. J. de; McHale, G.; I. Newton, M.; Roach, P.; J. Shirtcliffe, N. Nano-Scale Superhydrophobicity: Suppression of Protein Adsorption and Promotion of Flow-Induced Detachment. *Lab. Chip* **2008**, *8* (4), 582–586. https://doi.org/10.1039/B716509A.

(32) Wang, Z.; Zuilhof, H. Self-Healing Superhydrophobic Fluoropolymer Brushes as Highly Protein-Repellent Coatings https://pubs.acs.org/doi/abs/10.1021/acs.langmuir.6b01318 (accessed Oct 25, 2019). https://doi.org/10.1021/acs.langmuir.6b01318.

(33) Bartels, V. *Handbook of Medical Textiles*; Elsevier, 2011.

(34) Zhao, J.; Shi, Q.; Luan, S.; Song, L.; Yang, H.; Shi, H.; Jin, J.; Li, X.; Yin, J.; Stagnaro, P. Improved Biocompatibility and Antifouling Property of Polypropylene Non-Woven Fabric Membrane by Surface Grafting Zwitterionic Polymer. *J. Membr. Sci.* **2011**, *369* (1), 5–12. https://doi.org/10.1016/j.memsci.2010.10.046.

(35) Yu, Z.; Kastenmüller, G.; He, Y.; Belcredi, P.; Möller, G.; Prehn, C.; Mendes, J.; Wahl, S.; Roemisch-Margl, W.; Ceglarek, U.; Polonikov, A.; Dahmen, N.; Prokisch, H.; Xie, L.; Li, Y.; Wichmann, H.-E.; Peters, A.; Kronenberg, F.; Suhre, K.; Adamski, J.; Illig, T.; Wang-Sattler, R.

Differences between Human Plasma and Serum Metabolite Profiles. *PLoS ONE* **2011**, *6* (7). https://doi.org/10.1371/journal.pone.0021230.

(36) Norde, W.; Gage, D. Interaction of Bovine Serum Albumin and Human Blood Plasma with PEO-Tethered Surfaces: Influence of PEO Chain Length, Grafting Density, and Temperature. *Langmuir* **2004**, *20* (10), 4162–4167. https://doi.org/10.1021/la030417t.

(37) Top, J. F. Control of Adenovirus Acute Respiratory Disease in U.S. Army Trainees. *Yale J. Biol. Med.* **1975**, *48* (3), 185–195.

(38) Crawford-Miksza, L. K.; Nang, R. N.; Schnurr, D. P. Strain Variation in Adenovirus Serotypes 4 and 7a Causing Acute Respiratory Disease. *J. Clin. Microbiol.* **1999**, *37* (4), 1107–1112.

(39) Zhou, H.; Wang, H.; Niu, H.; Zhao, Y.; Xu, Z.; Lin, T. A Waterborne Coating System for Preparing Robust, Self-Healing, Superamphiphobic Surfaces. *Adv. Funct. Mater.* **2017**, *27* (14), 1604261. https://doi.org/10.1002/adfm.201604261.

(40) Golovin, K.; Boban, M.; Mabry, J. M.; Tuteja, A. Designing Self-Healing Superhydrophobic Surfaces with Exceptional Mechanical Durability. *ACS Appl. Mater. Interfaces* **2017**, *9* (12), 11212–11223. https://doi.org/10.1021/acsami.6b15491.

(41) Henry, B. J.; Carlin, J. P.; Hammerschmidt, J. A.; Buck, R. C.; Buxton, L. W.; Fiedler, H.; Seed, J.; Hernandez, O. A Critical Review of the Application of Polymer of Low Concern and Regulatory Criteria to Fluoropolymers. *Integr. Environ. Assess. Manag.* **2018**, *14* (3), 316–334. https://doi.org/10.1002/ieam.4035.

(42) Hintzer, K.; Schwertfeger, W. Fluoropolymers—Environmental Aspects. In *Handbook of Fluoropolymer Science and Technology*; John Wiley & Sons, Ltd, 2014; pp 495–520. https://doi.org/10.1002/9781118850220.ch21.

(43) Naftalovich, R.; Naftalovich, D.; Greenway, F. L. Polytetrafluoroethylene Ingestion as a Way to Increase Food Volume and Hence Satiety Without Increasing Calorie Content. *J. Diabetes Sci. Technol.* **2016**, *10* (4), 971–976. https://doi.org/10.1177/1932296815626726.

(44) Romanowski, E. G.; Yates, K. A.; Shanks, R. M. Q.; Kowalski, R. P. Benzalkonium Chloride Demonstrates Concentration-Dependent Antiviral Activity Against Adenovirus In Vitro. *J. Ocul. Pharmacol. Ther. Off. J. Assoc. Ocul. Pharmacol. Ther.* **2019**, *35* (5), 311–314. https://doi.org/10.1089/jop.2018.0145.

(45) Yates, K. A.; Shanks, R. M. Q.; Kowalski, R. P.; Romanowski, E. G. The In Vitro Evaluation of Povidone-Iodine Against Multiple Ocular Adenoviral Types. *J. Ocul. Pharmacol. Ther. Off. J. Assoc. Ocul. Pharmacol. Ther.* **2019**, *35* (2), 132–136. https://doi.org/10.1089/jop.2018.0122.

(46) Kennedy, M. A.; Parks, R. J. Adenovirus Virion Stability and the Viral Genome: Size Matters. *Mol. Ther. J. Am. Soc. Gene Ther.* **2009**, *17* (10), 1664. https://doi.org/10.1038/mt.2009.202.

(47) Young Thomas. III. An Essay on the Cohesion of Fluids. *Philos. Trans. R. Soc. Lond.* **1805**, *95*, 65–87. https://doi.org/10.1098/rstl.1805.0005.

(48) Yong, J.; Chen, F.; Yang, Q.; Huo, J.; Hou, X. Superoleophobic Surfaces. *Chem. Soc. Rev.* **2017**, *46* (14), 4168–4217. https://doi.org/10.1039/C6CS00751A.

(49) Hrncir, E.; Rosina, J. Surface Tension of Blood. *Physiol. Res.* **1997**, *46* (4), 319–321.

(50) Zozaya, J. A Physicochemical Study of Blood Sera. II: Analyses of Five Hundred Cases. *J. Phys. Chem.* **1937**, *42* (2), 191–207. https://doi.org/10.1021/j100897a004.

(51) Fowkes, F. M. Attractive Forces at Interfaces. *Ind. Eng. Chem.* **1964**, *56* (12), 40–52. https://doi.org/10.1021/ie50660a008.

(52) Kaewprasit, C.; Hequet, E.; Abidi, N.; Gourlot, J. P. Application of Methylene Blue Adsorption to Cotton Fiber Specific Surface Area Measurement: Part I. Methodology. **1998**, *2* (4), 10.

(53) Zhou, H.; Wang, H.; Niu, H.; Gestos, A.; Lin, T. Robust, Self-Healing Superamphiphobic Fabrics Prepared by Two-Step Coating of Fluoro-Containing Polymer, Fluoroalkyl Silane, and Modified Silica Nanoparticles. *Adv. Funct. Mater.* **2013**, *23* (13), 1664–1670. https://doi.org/10.1002/adfm.201202030.

(54) Bae, G. Y.; Min, B. G.; Jeong, Y. G.; Lee, S. C.; Jang, J. H.; Koo, G. H. Superhydrophobicity of Cotton Fabrics Treated with Silica Nanoparticles and Water-Repellent Agent. *J. Colloid Interface Sci.* **2009**, *337* (1), 170–175. https://doi.org/10.1016/j.jcis.2009.04.066.

(55) Zhu, Q.; Gao, Q.; Guo, Y.; Yang, C. Q.; Shen, L. Modified Silica Sol Coatings for Highly Hydrophobic Cotton and Polyester Fabrics Using a One-Step Procedure. *Ind. Eng. Chem. Res.* **2011**, *50* (10), 5881–5888. https://doi.org/10.1021/ie101825d.

(56) Jing, X.; Guo, Z. Biomimetic Super Durable and Stable Surfaces with Superhydrophobicity. *J. Mater. Chem. A* **2018**, *6* (35), 16731–16768. https://doi.org/10.1039/C8TA04994G.

(57) Choi, J.; Kim, T.-H.; Kim, H.-Y.; Kim, W. Ultrasonic Washing of Textiles. *Ultrason. Sonochem.* **2016**, *29*, 563–567. https://doi.org/10.1016/j.ultsonch.2015.07.018.

(58) Barraza, E. M.; Ludwig, S. L.; Gaydos, J. C.; Brundage, J. F. Reemergence of Adenovirus Type 4 Acute Respiratory Disease in Military Trainees: Report of an Outbreak during a Lapse in Vaccination. *J. Infect. Dis.* **1999**, *179* (6), 1531–1533. https://doi.org/10.1086/314772.

(59) Fowkes, F. M. Donor-Acceptor Interactions at Interfaces. *J. Adhes.* **1972**, *4* (2), 155–159. https://doi.org/10.1080/00218467208072219.

(60) Choi, J.; Jo, W.; Lee, S. Y.; Jung, Y. S.; Kim, S.-H.; Kim, H.-T. Flexible and Robust Superomniphobic Surfaces Created by Localized Photofluidization of Azopolymer Pillars. *ACS Nano* **2017**, *11* (8), 7821–7828. https://doi.org/10.1021/acsnano.7b01783.

TOC

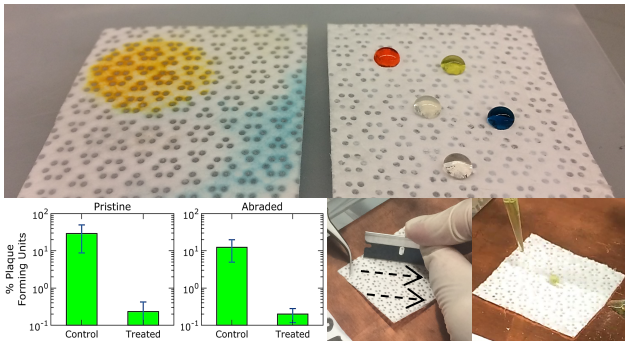
Pristine
Abraded
% Plaque Forming Units
Control
Treated
Control
Treated